Formation of Gold Nanoparticles by Laser Ablation in Aqueous Solution of Surfactant

Fumitaka Mafuné, Jun-ya Kohno, Yoshihiro Takeda, and Tamotsu Kondow*

Cluster Research Laboratory, Toyota Technological Institute, and East Tokyo Laboratory, Genesis Research Institute, Inc., 717-86 Futamata, Ichikawa, Chiba 272-0001, Japan

Hisahiro Sawabe

Central Technical Research Laboratory, Nippon Mitsubishi Oil Corporation, 8 Chidori-cho, Naka-ku, Yokohama 231-0815, Japan

Received: October 9, 2000; In Final Form: February 14, 2001

Gold nanoparticles were produced by laser ablation of a gold metal plate in an aqueous solution of sodium dodecyl sulfate. The absorption spectrum of the gold nanoparticles was essentially same as that of gold nanoparticles chemically prepared in a solution. The size distribution of the nanoparticles thus produced was measured by an electron microscope and was found to shift to a smaller size with an increase in surfactant concentration. This behavior is explained in terms of the dynamic formation model. Dependence of the nanoparticle abundance on surfactant concentration in the solution shows that stable gold nanoparticles tend to be formed as the surfactant concentration exceeds 10^{-5} M. The gold nanoparticles having diameters larger than 5 nm were pulverized into those having diameters of 1−5 nm by a 532-nm laser.

1. Introduction

Preparation of size-selected metal nanoparticles in a solution is one of the important subjects in chemistry and physics of nanoscale materials.[1−8] A considerable number of efforts have been directed for developing methods of their preparation such as chemical reduction of a metal salt in a micelle or a reversed micelle. On the analogy of the laser ablation for preparing gas-phase clusters,[9,10] on the other hand, Henglein, Cotton, and their co-workers have developed a laser ablation method for preparation of metal nanoparticles in a liquid.[11,12] More recently, Yeh and co-workers synthesized copper particles in 2-propanol by laser ablation of a copper oxide powder and characterized by using an electron microscope.[13] Takami and co-workers prepared small metal clusters by laser ablation of a metal plate in liquid helium, where the clusters are encapsulated in helium bubbles.[14−16]

In one of our previous papers, we prepared silver nanoparticles in an aqueous solution of sodium dedecyl sulfate (denoted SDS hereafter) by laser ablation against a silver plate.[17,18] We explained that a nanoparticle is formed via rapid formation of an embryonic silver particle followed by slow particle growth in competition with termination of the growth due to SDS coating on the particle. Actually, the size of the nanoparticles was found to decrease with an increase in the surfactant concentration and decrease with a decrease in the ablation laser power.[17] In addition, abundances of stable silver nanoparticles were further examined as functions of the concentration and the chain length of the surfactant, $C_nH_{2n+1}SO_4Na$ (n = 8, 10, 12, 16), and was found to depend strongly on both the concentration and the chain length: The abundance of the silver nanoparticles was maximized at the chain length of 12 and the concentration of 0.01 M.[18]

In the present study, we examined formation of gold nanoparticles by laser ablation of a gold metal plate in an aqueous solution of SDS, because they have an optical absorption in the vicinity of 532 nm, so that a further photoinduced effect is expected under the irradiation of the 532-nm laser.[19,20] The size and abundance of the gold nanoparticles were examined by changing the concentration of SDS and the wavelength of the ablation laser.

2. Experimental Section

Gold nanoparticles were produced by laser ablation of a metal gold plate in an aqueous solution of SDS. As shown in Figure 1, the metal plate (>99.99%) was placed on the bottom of a glass vessel filled with 10 mL of an aqueous solution of SDS. The metal plate was irradiated with an output of the fundamental (1064 nm) or the second harmonic (532 nm) of Quanta-ray GCR-170 Nd:YAG laser operating at 10 Hz, which was focused by a lens having a focal length of 250 mm. The spot size of the laser beam on the surface of the metal plate was varied in the range of 1−3 mm in diameter, by changing the distance between the focusing lens and the metal plate. A Scientech AC2501 power meter was used to monitor the laser power with a maximum output of about 90 mJ/pulse. Upon irradiation of the laser beam, the solution gradually turned to wine red. The absorption spectrum of the solution was measured by a Shimadzu UV-1200 spectrometer. At least five different runs were accumulated on an NEC computer to obtain one spectrum.

A transmission electron microscope (JEOL JEM-100S X50000) was employed to take the electron micrographs of the nanoparticles in the solutions studied. Practically, a drop of a sample solution was placed on a copper mesh coated with collodion and sputtered by ions in advance. The drop was dried by heating to 320 K. After repeating this procedure three times, the mesh was washed with water to remove free SDS. The diameters of more than 1000 nanoparticles in sight on a given micrograph were directly measured, and the distribution of the particle diameters (size distribution) was obtained.

* Corresponding author. E-mail: kondow@mail.cluster-unet.ocn.ne.jp.

10.1021/jp0037091 CCC: $20.00
Published on Web 05/11/2001

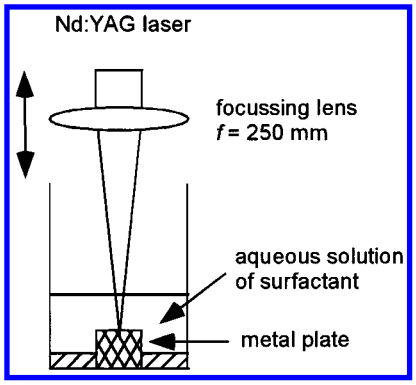

Figure 1. Schematic diagram of the experimental apparatus.

3. Results

Figure 2 shows electron micrographs and corresponding size distributions of gold nanoparticles produced by laser ablation at 1064 nm (80 mJ/pulse) of a gold plate immersed in a 0.01 M SDS aqueous solution; panels a and b show the electron micrographs of gold nanoparticles remaining in the top layer of the solution before and after centrifugation, respectively. The average nanoparticle diameter of 4.6 nm before centrifugation (panel a) is lowered to 4.0 nm after centrifugation (panel b). This result implies that a gold nanoparticle having a larger diameter is precipitated more efficiently by the centrifuge. Figure 3 shows gold nanoparticles and their size distributions produced in a 10^{-4} M SDS aqueous solution; panels a and b show the electron micrographs of the gold nanoparticles remaining in the top layer of the solution before and after centrifugation, respectively. The average diameters of the nanoparticles in panels a and b are 14.4 and 6.1 nm, respectively. The size distributions shown in Figures 2 and 3 indicate that gold nanoparticles having a larger diameter are precipitated by centrifugation, and as a result, the size distribution becomes narrow. In addition, the size of the nanoparticles was found to decrease with an increase in the concentration of SDS. Figure 4 shows optical absorption spectra of gold nanoparticles remaining in solution before (marked as a) and after centrifugation (marked as b). The spectra exhibit a characteristic peak at 517 nm and a tail portion of a broad band extending toward the UV wavelength range. The absorption spectra are essentially the same as that of gold nanoparticles prepared chemically by reduction of a gold salt in reversed micelles.[21] The agreement of the spectral features implies that gold nanoparticles are formed by the laser ablation in the solution. The dotted line marked as c in Figure 4 is the spectrum obtained by scaling spectrum b so that the absorbance of spectrum b agrees with that of spectrum a at the wavelength of 300 nm. The 517-nm peak of spectrum a is narrower and more intense than that of spectrum c. Figure 5 shows optical absorption spectra of gold nanoparticles produced at different concentrations of SDS in the solution. As shown in Figure 5, the 517-nm peak becomes broader and less prominent with an increase in the surfactant concentration. The peak broadening is attributed to the shift of size distribution of the produced gold nanoparticles, as discussed later.

The spectral feature in the 300−400 nm region did not change essentially except for the 517-nm peak, even when the condition of the particle preparation was changed (see Figures 4 and 5). The invariance of the spectral feature ensures that the relative absorbance at 300 nm can be employed as a measure of the relative abundance of gold nanoparticle in the solution. Figure 6 shows the relative abundances thus obtained plotted as a function of the concentration of SDS. In the lower concentration region ($<10^{-7}$ M), the relative abundance of the gold nanoparticles in the solution before the centrifugation (solid circles) does not change appreciably with the concentration of SDS, whereas the relative abundance increases with the concentration in the higher concentration region ($>10^{-5}$ M). On the other hand, the relative abundance of the gold nanoparticles in the solution after having the centrifugation (open circles) is almost zero below 10^{-6} M and starts to increase when the concentration exceeds 10^{-5} M.

The relative abundance of the gold nanoparticles in the solution is reduced from I_0 to $I_{\text{centrifuge}}$ by the centrifuge, because heavier and unstable nanoparticles tend to be precipitated. Let us define a precipitation fraction by having the centrifugation, $f_{\text{precipitation}}$, as

$$f_{\text{precipitation}} = (I_0 - I_{\text{centrifuge}})/I_0 \quad (1)$$

Figure 7 shows the precipitation fraction plotted as a function of the concentration of SDS in an aqueous SDS solution. The precipitation fractions both at 1064 nm (open circle) and at 532 nm (solid circle) decrease as the SDS concentration increases, although $f_{\text{precipitation}}$ at 532 nm is smaller than that at 1064 nm in the entire concentration range studied. In other words, the laser ablation at 532 nm produces more stable gold nanoparticles against the centrifuge.

Figure 8 shows the relative abundance of gold nanoparticles produced by laser ablation of the gold metal plate at 1064 nm (panel a) and 532 nm (panel b) as a function of a number of laser shots. The relative abundance of the gold nanoparticles increases almost linearly with the number of laser shots in panel a. In contrast, the relative abundance increases at first and levels off with the number of laser shots in panel b. The leveling-off feature is attributed to optical absorption of the ablation laser light by the nanoparticles suspended in the solution above the metal plate (see Figure 1).

Figure 9 shows an electron micrograph of gold nanoparticles and their size-distribution where the gold nanoparticles were produced by laser ablation at 1064 nm (80 mJ/pulse) of a gold plate immersed in a 0.01 M SDS aqueous solution and were irradiated by the 532-nm laser having a power of 50 mJ/pulse for 60 min. The gold nanoparticles having diameters larger than 5 nm were found to be pulverized into those having diameters of 1−5 nm by the irradiation of a 532-nm laser.

4. Discussion

4.1 Optical Absorption Spectrum. The optical absorption spectrum of gold nanoparticles exhibits one intense peak at 517 nm assignable to the surface plasmon on a tail part of a broad band originating from an interband transition.[22−29] An optical extinction coefficient of particles in a solution with smaller diameters than the wavelength of an incoming light (<500 nm) is basically given by the Mie theory, where the dielectric function can be written as a combination of an interband term related to the response of the d electrons and a Drude term for the conduction electrons in the particles. In a particle with a smaller diameter than the electron mean free path (~25 nm for gold), electron scattering at a particle boundary should be taken into account: Collision frequency of electrons in the particle, ω_c, increases with a decrease in the diameters. Practically, the size-dependent collision frequency, $\omega_c(R)$, is approximated by

$$\omega_c(R) = \omega_c + \upsilon_F/R \quad (2)$$

where ω_c (1.1×10^{14} s^{-1}) is the bulk collision frequency, υ_F (1.4×10^6 m s^{-1}) is the Fermi velocity, and R is the particle

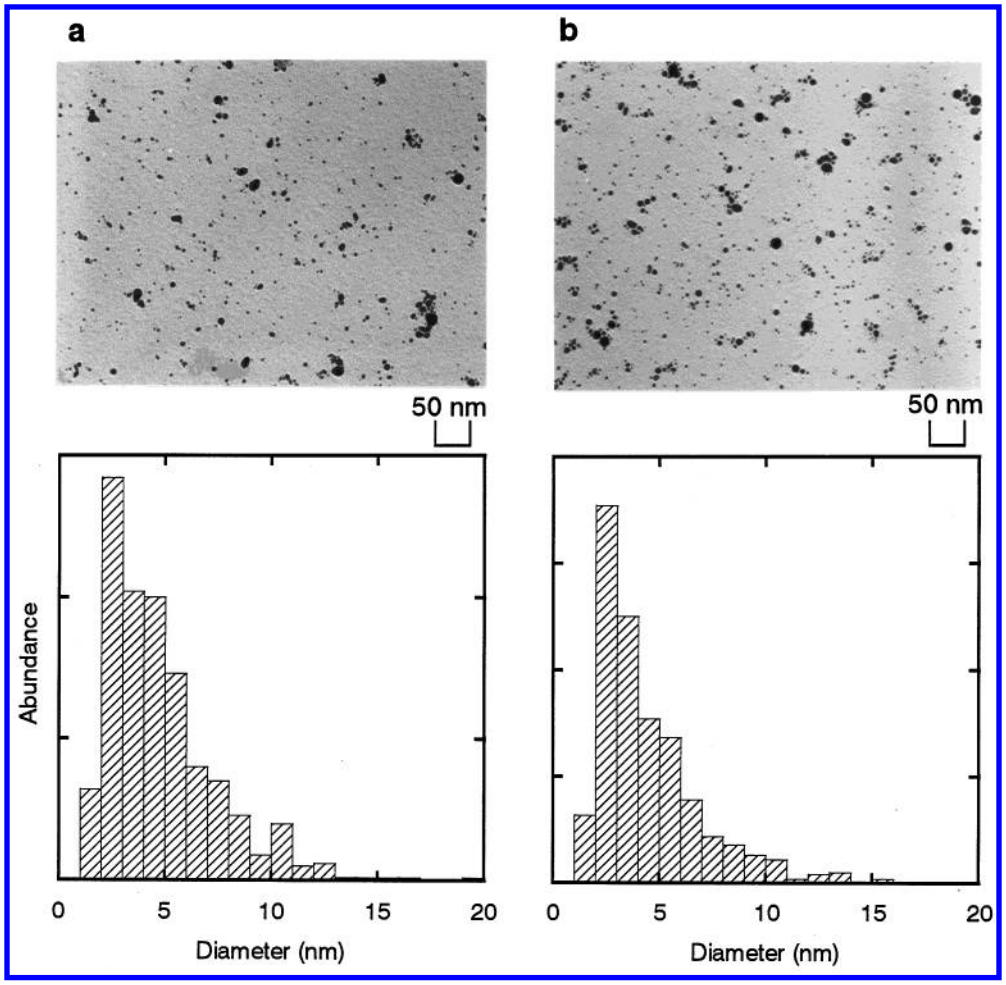

Figure 2. Electron micrographs and size distributions of the gold nanoparticles produced by 1064-nm laser ablation at 80 mJ/pulse in a 0.01 M SDS aqueous solution. Panels a and b show the electron micrographs of the gold nanoparticles remaining in the top layer of the solution before and after centrifugation, respectively.

radius.[27] The optical extinction coefficient of the gold particles in a solution was calculated as a function of the angular frequency of the incoming light and was found to reproduce the experimental one, where the parameters ω_p, ω_c, υ_F of a gold crystal and the diameter, R, measured by electron microscopy are employed.

As shown in Figure 2, the solution contains gold nanoparticles of 1−15 nm in diameter, and larger nanoparticles tend to be precipitated by the centrifuge. In other words, one can narrow the size distribution of nanoparticles in a solution by the treatment of the centrifuge. Therefore, the spectra shown in Figure 4a,b are regarded as that of an ensemble of widely distributed nanoparticles in diameter and that of an ensemble of nanoparticles with smaller diameters. From the spectra, one can recognize that the width of the surface plasmon peak centering at 517 nm increases with a decrease in the diameters.

The increase of the peak width shown in Figure 5 is ascribable to the reduction of the particle size due to the increase of the surfactant concentration. This behavior is explained in terms of the theory given above (see eq 2), where $\omega_c(R)$ increases linearly with the reciprocal of R.[25] This gives rise to broadening of the surface plasmon peak with an increase in the diameter of the nanoparticle.[3,29]

4.2 Formation Mechanism. As shown in Figures 2 and 3, the average diameter of the gold nanoparticles decreases with an increase in the concentration of SDS. The concentration dependence of size is supported by the optical absorption spectra: The surface plasmon peak at 517 nm in the absorption spectra tends to be broadened with the concentration of SDS (see Figure 5), as discussed in the previous section. The concentration dependence of size is explained in terms of the dynamic formation mechanism described in our previous paper;[17,18] rapid formation of an embryonic particle and a consecutive particle growth in competition with termination of the growth due to surfactant coating onto the particle. After the laser ablation, a dense cloud of gold atoms (plum) is built over the laser spot of the metal plate. The atoms are aggregated as fast as the atoms are supplied. This initial rapid aggregation continues until the atoms in close vicinity are depleted almost completely. As a result, an embryonic nanoparticle forms in a region void of the atoms. However, supply of the atoms outside the region through diffusion causes the particle to grow slowly even after the rapid growth ceases. The slow growth is terminated by coating the particle surface with SDS molecules, which diffuse through the solution toward the particle.

Let us define r_0 as the radius of the embryonic particle, V_a as the effective volume of a gold atom, and d_a as the number density of gold atoms in the cloud of the gold atoms. The radius of the particle, r_p, at a time, t, after the slow growth started is given by

$$r_p(t) = r_0 + (1/4)kV_a d_a \upsilon_a t \qquad (3)$$

where a gold atom is assumed to diffuse toward the particle with a velocity of υ_a, and $k\pi r_p^2$ is the attachment cross section of an atom to the particle. Here, we assume that the atoms

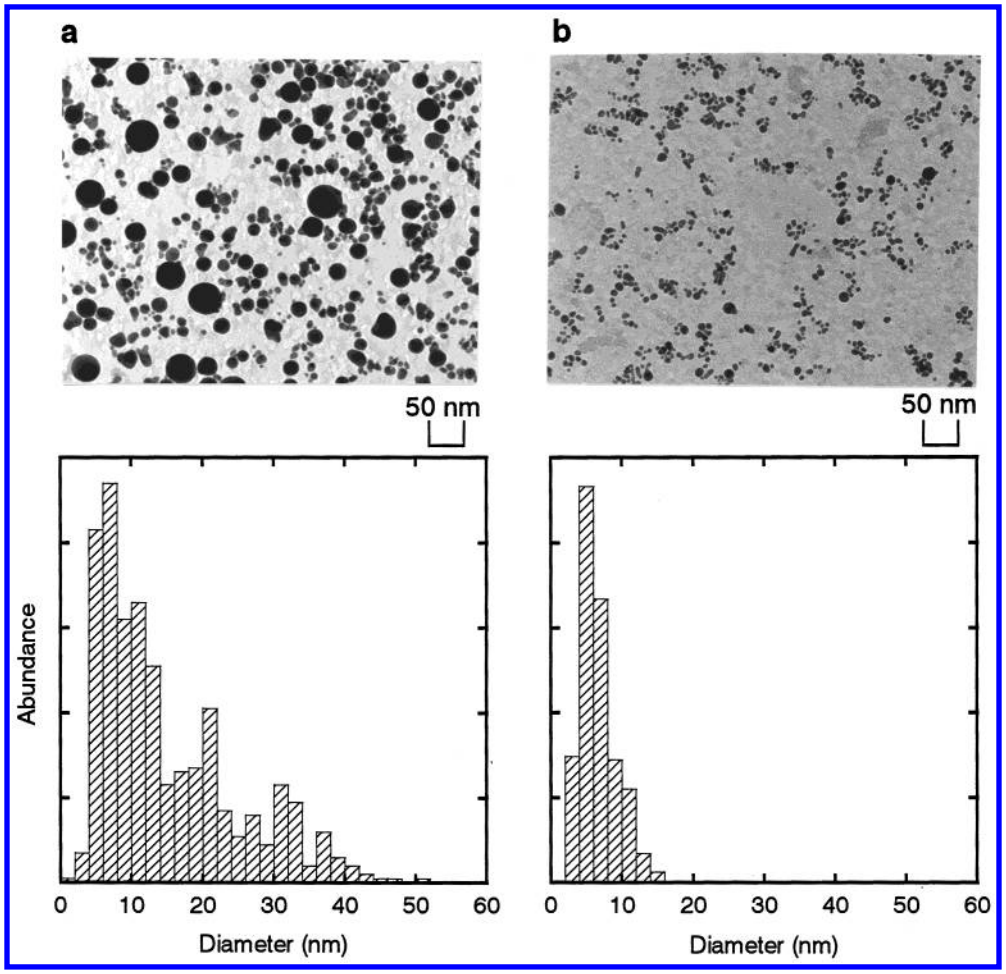

Figure 3. Electron micrographs and size distributions of the gold nanoparticles produced by 1064-nm laser ablation at 80 mJ/pulse in a 10^{-4} M SDS aqueous solution. Panels a and b show the electron micrographs of the gold nanoparticles remaining in the top layer of the solution before and after centrifugation, respectively.

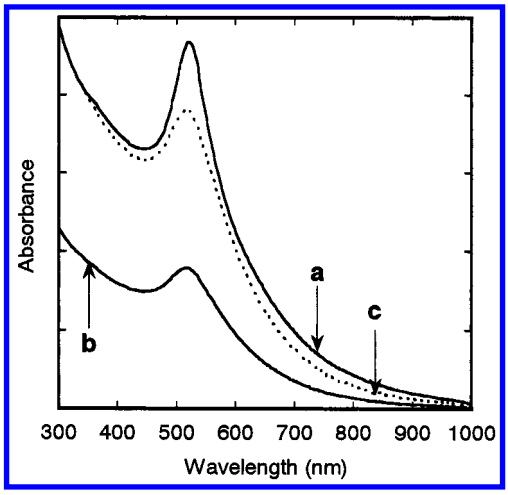

Figure 4. Optical absorption spectra of the nanoparticles produced by 1064-nm laser ablation at 80 mJ/pulse in a 0.01 M SDS solution. Solid lines a and b show the spectra of the gold nanoparticles remaining in the top layer of the solution before and after centrifugation, respectively. The dotted line c is obtained by normalization of line b so that the absorbances of spectra c and a coincide.

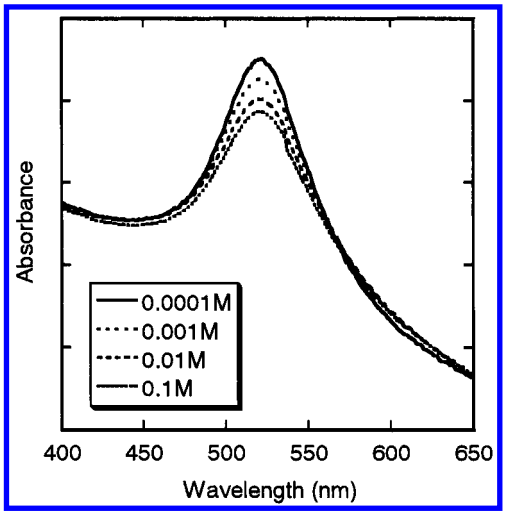

Figure 5. Optical absorption spectra of the gold nanoparticles produced by 1064-nm laser ablation at 80 mJ/pulse in 0.0001, 0.001, 0.01, and 0.1 M (from top to bottom) SDS aqueous solutions, respectively.

diffuse linearly with time, since only the atoms in the close vicinity of the embryonic particles attach to them. As shown in eq 3, the radius of the particle increases linearly with t.

Let us consider that a growing nanoparticle having a radius, r_s, at a time, t, is fully covered just at this time with SDS molecules that are diffusing toward the particle with the velocity of v_s. The radius, $r_s(t)$, is obtained as

$$r_s(t) = (S/3)^{1/2}(k' d_s v_s / k V_a d_a v_a)^{1/2}[(r_0 + (1/4)k V_a d_a v_a t)^3 - r_0^3]^{1/2} \quad (4)$$

where S is the surface area occupied by one SDS molecule on the particle, d_s is the number density of SDS molecules in a

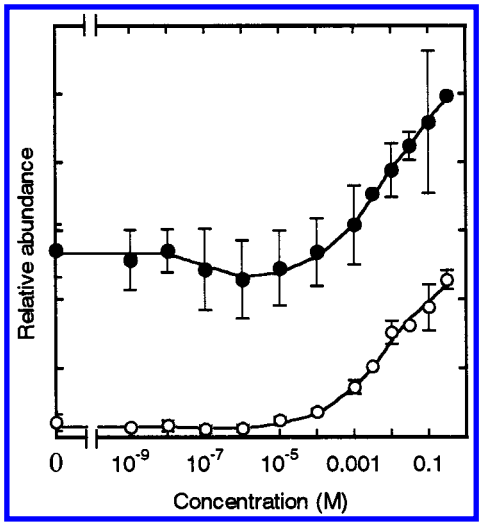

Figure 6. The relative abundance of the gold nanoparticles remaining in the solution before (solid circle) and after centrifugation (open circle) as a function of the SDS concentration, respectively. The gold nanoparticles were produced by 1064-nm laser ablation at 80 mJ/pulse.

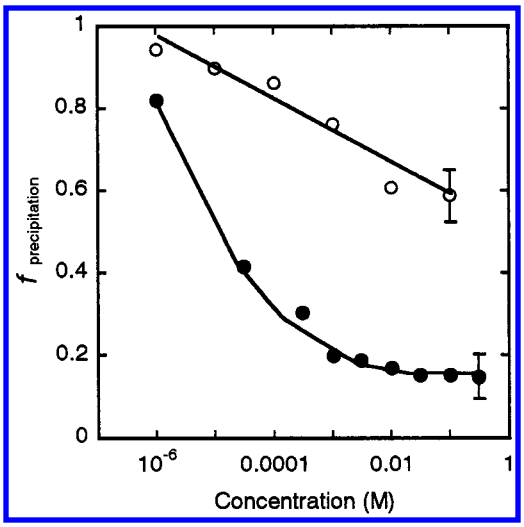

Figure 7. The precipitation fraction of the gold nanoparticles produced by 1064-nm laser ablation at 80 mJ/pulse (open circle) and by 532-nm laser ablation at 40 mJ/pulse (solid circle) as a function of the concentration of SDS in an aqueous solution.

solution and $k'\pi r_p^2$ represents the attachment cross section of an SDS molecule to the particle. Nanoparticles thus stabilized by the SDS coating on their surfaces appear at the time, t_s, when $r_p(t)$ is equal to $r_s(t)$; their diameter should be $r_p(t_s) = r_s(t_s)$.

Figure 10 shows the change of the calculated particle radius with a reduced time, kv_at, where V_a is calculated to be 1.70×10^{-29} m^3 from the radius of a gold atom in a gold crystal, and S of 6.5×10^{19} m^2 is taken from the literature.[30] In addition, the number density of the SDS molecules, d_s, is obtained from the SDS concentration, on the assumption that the SDS molecules are homogeneously distributed in the solution. The number of the gold atoms liberated into the solution per single laser shot is estimated to be $10^{11}-10^{12}$ from the absorbance of the gold nanoparticles in the region of the interband transition. The number density of gold atoms in the gold cloud, d_a, is estimated to be $10^{23}-10^{24}$ m^{-3} on the assumption that gold atoms ablated into the solution are thermalized immediately within a $\sim$1 μm diffusion length. The ratio, $k'v_s/kv_a$, is left as a variable parameter. As shown in Figure 10, the particle radius, r_p, increases linearly with the reduced time. On the other hand, the radius of the stabilized particle, r_s, increases more rapidly

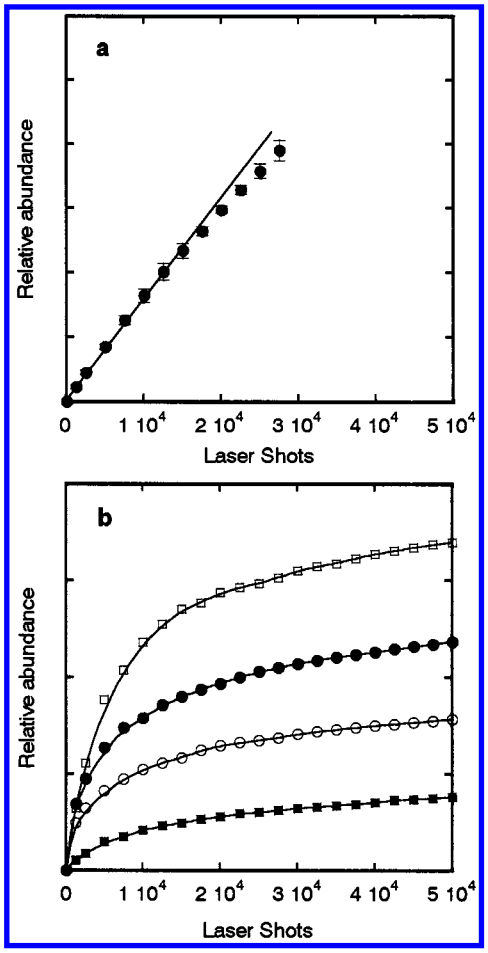

Figure 8. The relative abundance of the gold nanoparticles as a function of the laser shot at 1064 nm (panel a) and at 532 nm (panel b). In panel b, the laser powers were 20 mJ/pulse (solid square), 30 mJ/pulse (open circle), 40 mJ/pulse (solid circle), and 60 mJ/pulse (open square), respectively.

with the reduced time and exceeds at the reduced time of kv_at_s, where the two lines cross. This crossing point determines the average radius of the nanoparticles observed.

The size distribution of the gold nanoparticles implies that the average diameter of the embryonic gold particles is $\sim$4 nm ($r_0 \sim 2$ nm) and the SDS molecules attach to a gold nanoparticle by about 10 times faster than do the gold atoms ($k'v_s/kv_a \sim 10$). In a cloud of gold atoms produced by the laser ablation, a core made of a small number of gold atoms formed accidentally by density fluctuation in the cloud continue to grow until gold atoms in the vicinity ($\sim$40 nm) are consumed almost completely. The particle thus produced is the embryonic particle. The same growth mechanism is operative in silver nanoparticle formation in an aqueous solution of SDS by laser ablation onto a silver metal plate. However, silver atoms located more far away from the core ($\sim$100 nm) participate in the formation of the embryonic particle, because the interatomic interaction of silver is much stronger than that of gold.[17,18]

4.3 Structure and Stability of Nanoparticles. The concentration dependence of the abundance of the gold nanoparticles (see Figure 6) can be categorized into three regions according to their characteristic features: a low concentration region ($<10^{-7}$ M), a medium concentration region, and a high concentration region ($>10^{-5}$ M). In the low concentration region, the SDS concentration is so low that gold nanoparticles generated are scarcely covered with the SDS molecules. However, a sizable amount of gold nanoparticles are found to

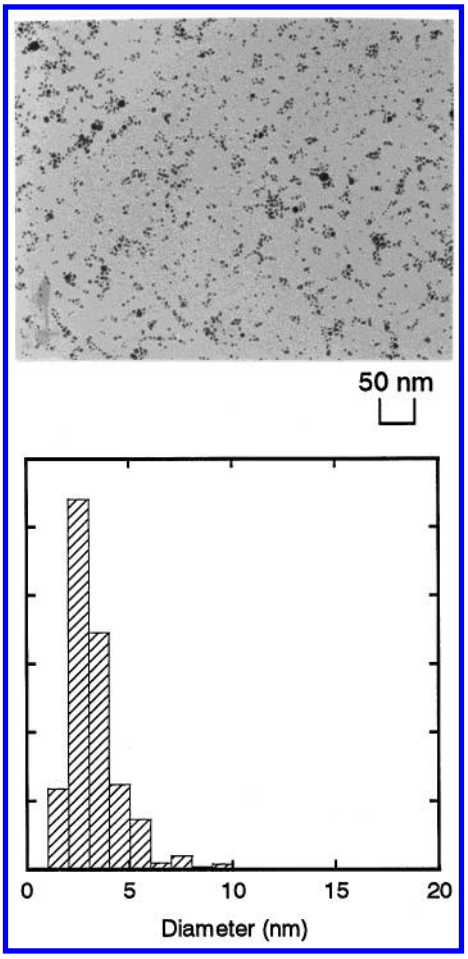

Figure 9. Electron micrograph and size distribution of the gold nanoparticles produced by 1064-nm laser ablation at 80 mJ/pulse in a 0.01 M SDS aqueous solution (the same condition as Figure 2a) and subsequent laser irradiation at 532 nm (50 mJ/pulse for 60 min.).

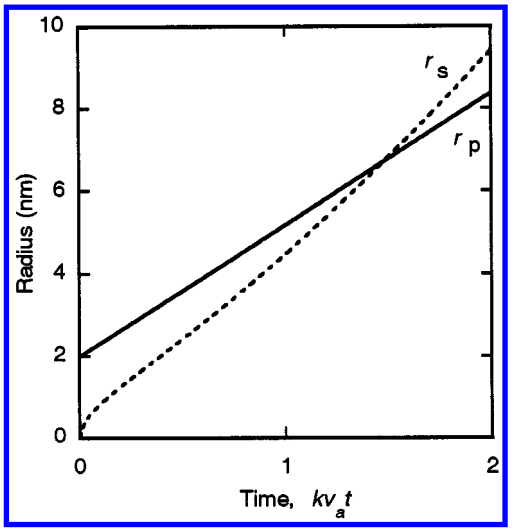

Figure 10. Time evolution of the particle radius, r_p (solid line) and r_s (dotted line), calculated on the basis of the dynamic formation model. The radius of the particle is calculated to be 6.7 nm when $r_0 = 2.0$ nm and $k'/k = 0.1$.

be suspended even in pure water, being independent of the SDS concentration. It is highly likely that the gold nanoparticles are positively charged, so that the particles are prevented from being coagulated by Coulomb repulsion exerted between the particles. Complete precipitation of the gold nanoparticles by centrifugation implies that the centrifugal force exceeds the Coulomb repulsion exerted between the nanoparticles.

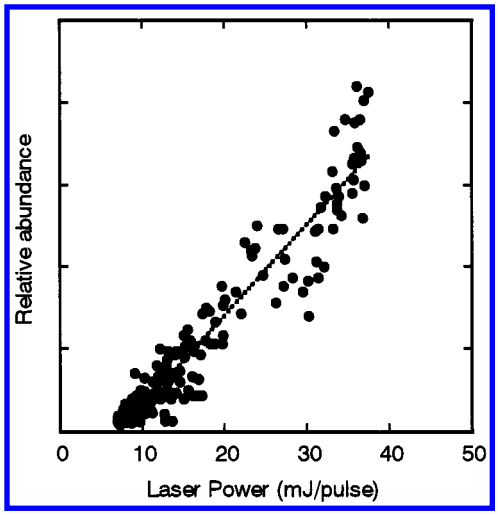

Figure 11. The relative abundance of the gold nanoparticles as a function of the laser power at 532 nm. The abundance starts to rise at a threshold laser power (7.2 ± 0.4 mJ/pulse) and increases almost linearly with the laser power.

In the medium region, the relative abundance before the centrifuge is lowered slightly. This phenomenon is interpreted in such a manner that gold nanoparticles present in the solution tend to be less charged by having their surfaces coated with SDS molecules and are inclined to be precipitated.

In the high concentration region ($>10^{-5}$ M), the relative abundance of the nanoparticles in the solution before the centrifugation increases with an increase in the SDS concentration. The relative abundance of the nanoparticles after the centrifugation increases similarly as well. This finding implies that the nanoparticles are increasingly stabilized with increase in the SDS concentration due to recharging their surfaces with forming a double layer of SDS. The neutralization and the recharging with an increase in the SDS concentration were examined whether or not the nanoparticles are dragged in a static electric field toward a cathode.

4.4 Photoabsorption by Nanoparticles. Figure 8a,b shows the relative abundances of the gold nanoparticles produced by laser ablation at 1064 and 532 nm as a function of the number of the laser shots, respectively. At 1064 nm, the relative abundance increases almost linearly with the laser shots in the initial stage, and its slope is slightly reduced above a laser shot of about 15 000. At 532 nm, on the other hand, the abundance of the nanoparticles increases and then levels off, as the number of the laser shot increases. This level off is considered to arise from absorption of the incident ablation laser by gold nanoparticles above the metal plate. Therefore, the apparent formation rate of the nanoparticles by the laser ablation decreases with an increase in the concentration of the nanoparticles in the solution. With the extinction rate of the light, ϵC, at 532 nm and a known optical length from the solution surface to the metal plate, l, the laser power reaching the metal surface, P, is given as

$$P = P_0 \times 10^{-\epsilon C l} \tag{5}$$

where P_0 is the power of the incident ablation laser. Figure 11 shows the abundance of the nanoparticles per 500 shots as a function of the laser power thus obtained, P. The abundance starts to rise at a threshold laser power, (7.2 ± 0.4 mJ/pulse) and increases almost linearly with the laser power: the diameter of the laser spot was ~2 mm. The existence of the threshold

laser power for the formation of the nanoparticles ($\sim 4 \times 10^7$ W/cm^2) shows that a certain laser power is needed for the ablation of the metal plate.

4.5 Photofragmentation of Nanoparticles in a Solution. The nanoparticles in the solution do not absorb photons at 1064 nm, but those absorb photons at 532 nm and fragment into the smaller nanoparticles. Dissociation of the gold nanoparticles by absorption of 532-nm photons was proved by an experiment that gold nanoparticles are at first prepared by the laser ablation at 1064 nm and then are irradiated with the 532-nm laser. Actually, the nanoparticles were found to be dissociated into smaller nanoparticles with a narrow size distribution (see Figure 9). The present result is consistent with the results of Koda and co-workers, who have shown that chemically prepared gold nanoparticles in a solution are dissociated into smaller particles (photoinduced reshaping) under irradiation of a 532-nm laser.[30]

Smaller nanoparticles produced by the photofragmentation are more resistant against the centrifugal force, and accordingly, the precipitation fraction decreases in the entire concentration range studied (see Figure 7): The monotonic decrease of the precipitation fraction is consistent with the present explanation that the nanoparticles tend to be more completely covered by a double layer of SDS in a more concentrated SDS solution. At 10^{-5} M where the nanoparticles are incompletely covered by the double layer of SDS, the precipitation fraction of the nanoparticles produced at 532 nm is slightly smaller than those produced at 1064 nm, although the size of the nanoparticles produced by the 532-nm laser is much smaller than that produced at 1064 nm. In contrast, at 0.1 M where the nanoparticles are almost fully covered by the double layer of SDS, the precipitation fraction at 532 nm is smaller than that at 1064 nm. This finding implies that the stability of the nanoparticles in the solution against the centrifuge more strongly depends on the coverage by the SDS molecules than the size.

5. Conclusions

Laser ablation of a metal plate in an aqueous solution of SDS was used to prepare gold nanoparticles in the solution. The produced nanoparticles were characterized by optical-absorption spectroscopy, electron microscopy, and centrifugation. The size distribution of the nanoparticles was found to shift smaller with increase in the concentration of SDS, and the concentration dependence was explained in terms of the dynamic formation model. Size selection of the gold nanoparticles within 1−5 nm in diameter was performed by using centrifugation and photo-induced reshaping. This method is applicable to prepare metal nanoparticles of any kind including multicomponent ones.

Acknowledgment. This work is financially supported by the Special Cluster Research Project of Genesis Research Institute, Inc.

References and Notes

(1) Enustun B. V.; Turkevich, J. J *J. Am. Chem. Soc.* **1963**, *85*, 3317.
(2) Kortenaar, M. V. t.; Kolar, Z. I.; Tichelaar, F. D. *J. Phys. Chem. B* **1999**, *103*, 2054.
(3) Petit, C.; Lixon, P.; Pileni, M. P. *J. Phys. Chem.* **1993**, *97*, 12974.
(4) Pileni M. P. *Nanostructured Materials*; Shalaev, V. M., Moskovits, M., Eds.; American Chemical Society: Washington, 1997.
(5) Pileni, M. P. *Langmuir* **1997**, *13*, 3266.
(6) Baker, B. E.; Kline, N. J.; Treado, P. J.; Naten, M. J. *J. Am. Chem. Soc.* **1996**, *118*, 8721.
(7) Grabar, K. C.; Smith, P. C.; Musick, M. D.; Davis, J. A.; Walter, D. G.; Jackson, K. C.; Guthrie, A. P.; Naten, M. J. *J. Am. Chem. Soc.* **1996**, *118*, 1148.
(8) Petroski, J. M.; Wang, Z. L.; Green, T. C.; El-Sayed, M. A. *J. Phys. Chem. B.* **1998**, *102*, 3316.
(9) Maruyama, S.; Anderson, L. R.; Smalley, R. E. *Rev. Sci. Instrum.* **1990**, *61*, 2427.
(10) Milani, P.; deHeer, W. A. *Rev. Sci. Instrum.* **1990**, *61*, 1835.
(11) Fojtik, A.; Henglein, A. *Ber. Bunsen-Ges. Phys. Chem.* **1993**, *97*, 252.
(12) Sibbald, M. S.; Chumanov, G.; Cotton, T. M. *J. Phys. Chem.* **1996**, *100*, 4672.
(13) Yeh.. M. S.; Yang, Y. S.; Lee, Y. P.; Lee, H. F.; Yeh, Y. H.; Yeh, C. S. *J. Phys. Chem. B* **1999**, *103*, 6851.
(14) Persson, J. L.; Hui, Q.; Nakamura, M.; Takami, M. *Phys. Rev. A* **1995**, *52*, 2011.
(15) Hui, Q.; Parsson, J. L.; Beijersbergen, J. H. M.; Takami, M. *Z. Phys. B* **1995**, *98*, 353.
(16) Jakubek, Z. J.; Hui, Q.; Takami, M. *Phys. Rev. Lett.* **1996**, *79*, 629.
(17) Mafuné, F.; Kohno, J.; Takeda, Y.; Kondow, T.; Sawabe, H. *J. Phys. Chem. B* **2000**, *104*, 8333.
(18) Mafuné, F.; Kohno, J.; Takeda, Y.; Kondow, T.; Sawabe, H. *J. Phys. Chem. B* **2000**, *104*, 9111.
(19) Jurita, H.; Takami, A.; Koda, S. *Appl. Phys. Lett.* **1998**, *72*, 789.
(20) Takami, A.; Kurita, H.; Koda, S. *J. Phys. Chem. B* **1999**, *103*, 1226.
(21) Alvarez, M. M.; Khoury, J. T.; Schaaff, T. G.; Shafigullin, M. N.; Vezmar, I.; Whetten, R. L. *J. Phys. Chem. B* **1997**, *101*, 3706.
(22) Charle, K.-P.; Schulze, W. *Clusters of Atoms and Molecules II*; Haberland, H., Ed.; Springer: Tokyo, 1994.
(23) Bohren, C. F.; Huffman, D. R. *Absorption and Scattering of Light by Small Particles*; Wiley: New York, 1983.
(24) Doremus, R. H. *J. Chem. Phys.* **1964**, *40*, 2389.
(25) Kreibig, U.; Fragstein, C. v. *Z. Physik* **1969**, *224*, 307.
(26) Kreibig, U. *J. Phys. F* **1974**, *4*, 999.
(27) Gramqvost, C. G.; Hunderi, O. **1977**, *16*, 3513.
(28) Charle, K.-P.; Frank, F.; Schulze, W. *Ber. Bunsen-Ges. Phys. Chem.* **1984**, *88*, 350.
(29) Link, S.; El-Sayed, M. A. *J. Phys. Chem. B* **1999**, *103*, 8410.
(30) Israelachvili, J. N. *Intermolecular and Surface Forces*; Academic Press: New York, 1985.